Theor Chem Acc (2012) 131:1221
DOI 10.1007/s00214-012-1221-z

REGULAR ARTICLE

Effects of mutations on the absorption spectra of copper proteins: a QM/MM study

Antonio Monari · Thibaut Very · Jean-Louis Rivail · Xavier Assfeld

Received: 9 February 2012 / Accepted: 8 April 2012 / Published online: 25 April 2012

Abstract The ground and excited state properties of copper proteins are studied and analyzed using hybrid quantum mechanics/molecular mechanics technique. Wild-type plastocyanin, characterized by an intense blue color, and wild-type nitrosocyanin, a red protein, are considered. These proteins differ from some ligands of the copper containing chromophore; we also studied the effects of selective mutations of one of the active site residue in plastocyanin. It is shown that this mutation is able to strongly modify the UV/VIS spectrum continuously modifying the absorption spectrum of the protein that from blue becomes red. Electrostatic and polarization effects of the macromolecular environment on the chromophore are taken into account using original techniques. Principal transitions are analyzed by mean of natural transition orbitals.

Keywords QM/MM · TD-DFT · Absorption spectra · Copper protein

Dedicated to Professor Marco Antonio Chaer Nascimento and published as part of the special collection of articles celebrating his 65th birthday.

Electronic supplementary material The online version of this article (doi:10.1007/s00214-012-1221-z) contains supplementary material, which is available to authorized users.

A. Monari (✉) · T. Very · J.-L. Rivail (✉) · X. Assfeld
Equipe de Chimie et Biochime Théoriques, SRSMC-UMR 7565, Université de Lorraine-Nancy and CNRS, BP-70239, 54506 Nancy-Vandoeuvre, France
e-mail: antonio.monari@cbt.uhp-nancy.fr

J.-L. Rivail
e-mail: Jean-Louis.Rivail@cbt.uhp-nancy.fr

1 Introduction

Among the many metalloproteins, copper proteins occur in a wide variety of biological systems, ranging from bacteria to humans [1–3]. In particular, plastocyanins (see Fig. 1) play a very important role as electron carriers during the photosynthesis process in higher plants. They contain a copper II ion and are reduced by cytochrome f of photosystem II [1]. The reduced form in which the extra electron is mainly located on the copper ion can transfer an electron to photosystem I [4, 5]. This class of plastocyanins can be found in many superior plants; the difference between them comes from few structural modifications from species to species. More important mutations give rise to the class of azurine, found in bacteria. The latter proteins start to show a great interest as antitumoral agents [6].

It is striking to notice how much the physicochemical properties of these compounds differ from those of aqueous copper complexes [7–12]. In particular, they exhibit an anomalously high reduction potential and usually a very intense absorption band in the visible range, which shifts from a compound to another. The role of the protein appears to be crucial in these changes, and it is twofold. First, it constrains the geometry of the coordination arrangement of the copper ion, and second, the various residues entering this coordination sphere can induce important changes in these physicochemical properties. Indeed, several such plastocyanins differ from a parent one by a mutation in the coordination arrangement. Finally, artificial mutations can be imposed in order to tune some property of interest [13], or in some cases, equilibrium between green and blue form has been reported [14].

Many theoretical investigations on such systems have been performed [15–25] in the past, and recently some

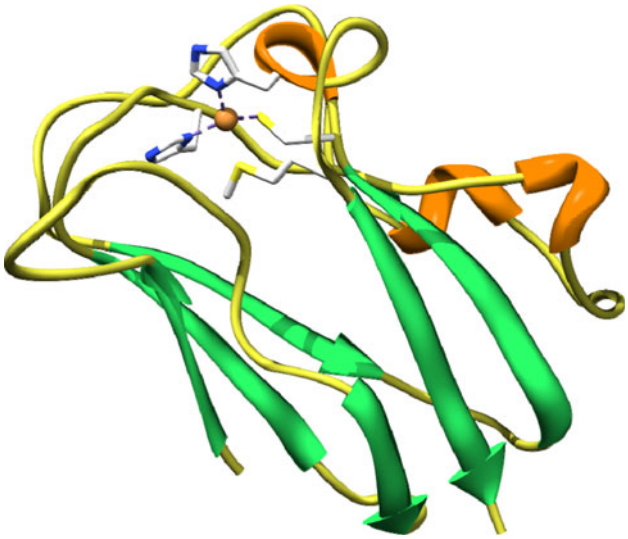

Fig. 1 The structure of plastocyanin, active site in ball and stick representation

mixed ab initio molecular dynamics and Car Parrinello dynamical studies have been reported [22–25].

In a previous paper [26], we have shown that a mixed quantum mechanics/molecular mechanics (QM/MM) approach of the spinach plastocyanin is quite appropriate to address the spectroscopic as well as the redox properties of this molecule and to analyze the influence of the various characteristics of the macromolecular surroundings on these properties. In the present paper, we focus our attention on the influence of the changes of the copper II fourfold coordination on the spectroscopic properties by considering the mutations of the methionine residue by the cysteine anion, cysteine, glutamate and homocysteine anion. We also considered the case of nitrosocyanin [27–30] (see Fig. 2), which is an example of a system in which the copper ion is surrounded by five ligands. Indeed,

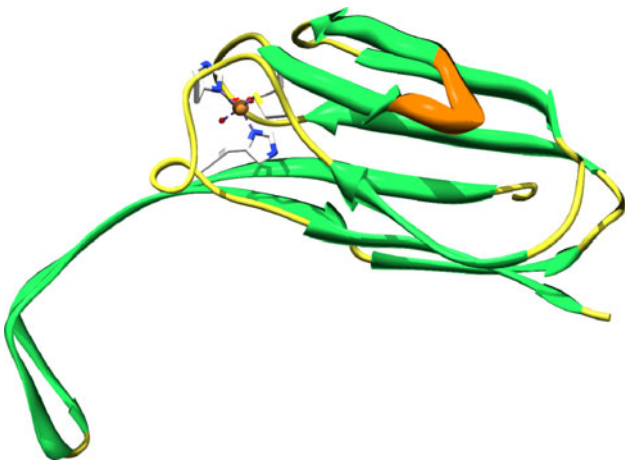

Fig. 2 The structure of nitrosocyanin, active site in ball and stick representation. Note the water molecule coordinating to copper

nitrosocyanin, the structure of which was resolved much more recently [27, 28], has a still unclear biological role, and contrary to plastocyanin, it exhibits an intense red color. The two proteins can be clearly related, and both show a quite rigid secondary structure, dominated by a β-sheet motif, with the chromophore being placed in a relative peripheral region. The active sites of both systems, see Fig. 3, show quite important similarities between them; in particular in both cases, two histidines are present as ligands, as well as one cysteine anion. The most important difference is the replacement of the relatively weak ligand methionine by a glutamate anion capable of a much more important interaction. As previously said, this reorganization of the active site leaves a free position in the coordination sphere of the copper II ion that is usually filled with a water molecule, therefore, leading to a pentacoordinate structure. Copper II ion bears, in both cases, an unpaired electron, mainly centered on metal but exhibiting quite an important delocalization over the different ligands in particular with the cysteine residue, as confirmed for instance by electron spin resonance (ESR) spectrum.

Recently, the effect of the mutation of the methionine ligand on the absorption spectrum of the blue-copper proteins has been underlined and proved experimentally [13], as well as the artificial mutation of the active site loop sequence of plastocyanin with the nitrosocyanin one giving rise to a red-copper protein [31].

In the present article, the absorption properties of the two native proteins, as well as the ESR and circular dichroism (CD) parameters, will be analyzed, at density functional theory (DFT) and time-dependent DFT (TD-DFT) level. The use of hybrid QM/MM approach will allow us to take into account the role of the macromolecular environment [32–37]. The evolution of the spectroscopic parameters with mutations will be also considered. The use of natural transition orbitals (NTOs) [26, 38] techniques will allow us to perform a systematic analysis of the nature and electronic properties of the excited states,

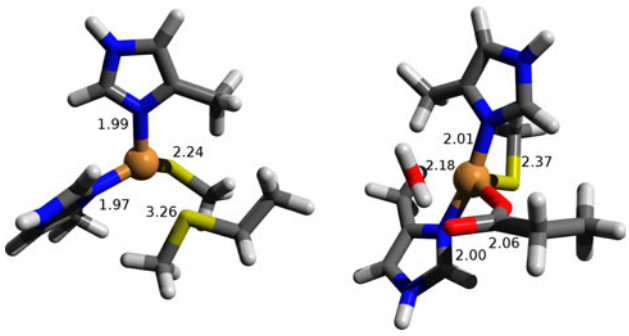

Fig. 3 The optimized active site of plastocyanin (*left*) and nitrosocyanin (*right*) in stick representation. The distances between the metal ion and the ligands are reported

allowing a systematic comparison of the different spectroscopic properties.

The present article is organized as follows: in Sect. 2, we present the computational strategy and details used in the present work, Results are analyzed and discussed in Sect. 3, and finally conclusion is drawn in Sect. 4.

2 Computational details and strategy

In order to correctly treat the macromolecular environment, we have partitioned our system in two regions: the active site treated at QM level and the outer region treated at MM level. Hybrid QM/MM computations have been performed using a local modified version of Gaussian 09 code [39], in which the local self-consistent field technique (LSCF) [40, 41] has been implemented. The coupling with MM has been performed by a local modified version of the Tinker code [42].

2.1 Computational strategy

Native proteins structures have been retrieved from the Protein Data Bank (PDB), blue-copper spinach plastocyanin is identified by the PDB code as 1AG6 (crystallographic resolution of 1.70 Å), while red-copper nitrosocyanin derived from the nitrifying bacterium *Nitrosomonas Europea* has the code 1IC0 (resolution of 1.65 Å). Nitrosocyanin crystallizes as a tetramer and, in order to simplify the computational problem, only one monomer of the protein has been considered. Mutated proteins have been constructed starting from the native plastocyanin by substitution of the Met91 residue, with cysteine, deprotonated cysteine, glutamate and the non-proteinogenic homocysteine aminoacid. The MM part of the system has been modeled by using CHARMM [43] force field parameters, as previously done for the study of plastocyanin. The QM/MM frontier has been located on the C_α–C_β bond of each of the four aminoacids directly interacting with the copper atom: His3, His86, Cys83, Met91 for plastocyanin and Glu60, Cys95, His98, His103 for nitrosocyanin.

The QM part was therefore composed of the copper II ion and of the lateral chains of the four aminoacids for plastocyanin. In the case of nitrosocyanin, an extra water molecule has been added to fill the vacancy in the coordination sphere. The effects of the MM point charges on the QM wavefunction have been directly taken into account by means of the so called electrostatic embedding, that is, by their inclusion into the QM Fock operator [40, 41].

In all the cases, the QM active site has been optimized, also allowing the geometry relaxation of the neighboring MM aminoacids. During the geometry optimization, a LANL2DZ [42–46] basis including pseudopotential for copper has been used together with B3LYP [47, 48] hybrid exchange and correlation functional. The frontier bonds have been treated by means of strictly localized bonding orbitals (SLBO) [40, 41] placing a doubly occupied local orbital, obtained from a model system (ethane), on each frontier bond. Subsequently, the LSCF technique [40, 41] was used to optimize the wavefunction under the constrain due to the SLBO, following a strategy that already proved efficiently in the calculations of biological systems.

Once the system has been optimized, excited states have been obtained at TD-DFT [38, 49] level in order to model absorption and circular dichroism spectra. In this case, we still used B3LYP exchange functional but the basis set was changed to a 6-31+G(d,p) set [50–52] in order to take into account the effect of diffuse functions. For these calculations, the frontier was treated using link-atoms (LA) technique [40, 41], that is, capping the dangling bond with an hydrogen atom, since the use of diffuse functions could produce unphysical transition on the frontier atoms when using SLBO techniques. Notice that when computing the UV/VIS spectra with the LANL2DZ basis, LA or SLBO techniques give absolutely superimposable results. CD spectra intensities [53, 54] have been obtained computing the rotatory strength by means of the "velocity" algorithm; the "length" formalism although showing a similar behavior gave the wrong sign for some of the less intense transitions. Finally, note that in order to match experimental results, vertical transitions have been convoluted with Gaussian functions of fixed half-length width of 0.2 eV. As previously reported [26] we underline that, although dealing with charge transfer transitions, in isolated model systems similar to our active site, the use of long range corrected functional gives practically indistinguishable spectra. To be assured of such an occurrence, we also performed more tests computing the absorption spectrum of the isolated plastocyanin active site (at the QM/MM B3LYP optimized geometry) using three more functionals: CAM-B3LYP [55], wB97XD [56], PBE0 [57]. The difference on the excitation energies of the most intense transitions with respect to the B3LYP results does not exceed 0.02 eV. This is probably due to the dimension of the active site and strongly justifies our choice to perform all the subsequent computations with B3LYP functional, only.

The ESR parameters, mainly the g-factors and the isotropic hyperfine A values, have also been obtained using the 6-31+G(d,p) basis set; rough g-factors tensor has been diagonalized in order to better compare the experimental data.

2.2 Electrostatic polarization of the MM part

When dealing with the modification induced on the UV/VIS spectra of a chromophore embedded in a macromolecular environment, one has to take into account three main effects: the geometric deformation induced by the rather rigid environment, the electrostatic effect modeled by the polarization of the wavefunction induced by the MM point charges, and finally the electronic polarization of the environment due to the modification of the electronic density of the environment to adapt itself to the new excited state electronic density.

The electrostatic effects can be easily taken into account by using electrostatic embedding in the QM/MM calculations. Conversely, the influence of the fixed charges on classical atoms can be easily evidenced by setting them to zero and performing another QM computation on the previously optimized fixed geometry. The electronic response of the surroundings (ERS) [26, 31–34] technique allows us to simulate the role of electronic polarization, that is, the modifications of the electronic distribution of the classical subsystem treated at MM level under the influence of the density modification in the QM part. Indeed, if within the framework of the Franck–Condon principle, the electronic transitions are vertical and do not involve any nuclear position rearrangement, the electronic cloud of the environment can, however, instantaneously adapt itself to the new electronic distribution of the chromophore. Since the electrons of the MM part are not treated explicitly, different possibilities exist to take this phenomenon into account. One solution consists in using polarizable force fields. Although rigorous, and able to take into account all the anisotropies of the environment, this choice suffers the drawback of a consequently augmented computational cost. Moreover, the use of polarizable force fields is nowadays not a standard task and can be quite problematic. In the framework of ERS technique, we model the electronic response of the environment by means of a polarizable continuum medium characterized by a dielectric constant extrapolated at infinite frequency. Technically, the chromophore is placed in a site cavity created in the continuum and the MM points charges of the protein do not interact with the continuum. ERS technique already proved its efficiency in modeling the important effects of electronic polarizability on the position and intensities of electronic transitions, at a very moderate additional computational cost [26, 31–34].

2.3 Natural transition orbitals

One of the most useful features of excited state computation rests in the possibility of making an accurate analysis of the excited states in terms of electron density rearrangement with respect to the ground state. Indeed, in linear response TD-DFT formalism, one can express excited states as a linear combination of single-electron excitation from occupied to virtual Kohn–Sham orbitals. If in some cases, such an analysis is straightforward, since the excited state is dominated by only one excitation, there are cases in which many couples of orbitals are participating to the expansion with a similar weight, therefore making the analysis quite cumbersome. To overcome such a problem, one can use the so called NTOs [26, 38, 58], based on a unitary transformation of the 1-electron transition density matrix **T**. Indeed, NTOs are obtained by a singular value decomposition of the **T** matrix, leading to two matrices **U** and **V** storing occupied and virtual NTOs, respectively. The singular values **Λ** represent the weight of the transition from an occupied to the corresponding virtual orbital. In contrast with the molecular orbitals representation, only one, or in the worst cases two, transitions dominate the expansion and the description of the excited states, making the analysis much simpler. Speaking in more physically terms, one can think of the dominant occupied NTOs as of the orbital from which the electron is taken away upon the excitation, that is, representing a sort of hole density, while the virtual one represents the orbital that describes the electron rearrangement in the excited states. NTOs have been obtained by a postprocessing of gaussian 09 transition densities using a code specifically designed and produced in our laboratory. The code, licensed under gnu public license, is free and can be downloaded from http://nancyex.sourceforge.net [26].

3 Results and discussion

In this Section, we will analyze and compare the results obtained for plastocyanin and nitrosocyanin, in terms of chromophore structure, UV/VIS and circular dicroism spectrum and ESR parameter.

3.1 Structural parameters

The QM/MM optimized active site for plastocyanin and nitrosocyanin is represented in Fig. 3 (left and right panel, respectively); more structural parameters are reported in Supplementary Materials. One can immediately see that in the case of Copper II plastocyanin, the active site assumes a distorted tetrahedral arrangement with three ligands much more strongly bonded than methionine. Indeed, as already underlined computationally [22–26] and experimentally [1–6], the Cu–Met distance is quite large and close to 3.50 Å; conversely, the Cu–Cys bond length is quite shorter going to 2.20 Å. The angles comprising methionine also appears noticeably distorted with the Met–Cu–His angle being close to 90°.

The structure of nitrosocyanin appears quite different, and the geometry, when we include the water molecule, appears much closer to a trigonal bipyramid. Indeed, the two histidines act like the apical ligands, the angle between the two nitrogen atoms and copper ion being close to 180°, on the other hand, the anionic glutamate and cysteine, together with water, can be considered as the three equatorial ligands, roughly lying on the same plane. As the distances are concerned, we can see that the Cys–Cu bond length is only slightly perturbed but is lengthened to the value of 2.37 Å. On the contrary, the carboxylic group of the glutamate ion is much closer to the metal, the closest oxygen atom being at a distance of 2.06 Å only from copper. This aspect reveals a totally different role played by such a residue compared to methionine in plastocyanine. On the other hand, the distances between the histidine nitrogen atom and the copper ion are still close to 2.00 Å and not too much changed compared to the case of blue plastocyanin. Finally, as the water molecule is concerned, the distance between oxygen and copper is quite a common one of 2.18 Å. If we consider the angles between ligands, as already stated, the two histidines forming the apical ligands the N–Cu–N angle has a value of about 170°, the angles between the equatorial ligands are indeed much more distorted and vary from about 89° (water–Cu–Glu) to 160° (water–Cu–Cys). This deviation can also be ascribed to the possibility for the water molecule to come closer to the second oxygen of glutamate to be stabilized by a hydrogen bond. Indeed, the distance between the hydrogen of water and glutamate oxygen is of 1.62 Å.

Of course when mutations are introduced in the plastocyanin active site, structural deformations appear to be less important in magnitude than for the nitrosocyanin case. The distorted tetrahedral site is preserved, the most affected parameter being the distance between the mutated residue and the copper ion. In the case of protonated and deprotonated cysteine, the Cu–S distance for the mutated residue remains quite large and greater than 4.50 Å. This peculiarity can be explained also by the fact that cysteine has a lateral chain shorter than methionine. Therefore, the protein backbone geometric constrain keeps the cysteine residue quite far from the copper ion, even when deprotonation occurs. This is confirmed when one looks at the homocysteine case. This aminoacid has a lateral chain constituted by two CH_2 groups bonded to a SH function, its length is therefore comparable to that of methionine, but the presence of the anion centered on the S atom should lead to a much stronger interaction. Indeed, the Cu–S distance is reduced to 2.40 Å and becomes equivalent to the Cu–S distance of the native cysteine, leading to a much more symmetric arrangement. Finally, in the case of glutamate, the C–O distance is much shorter and goes down to 2.00 Å, indicating a much stronger interaction with the metal ion.

3.2 Ground state electronic structure and ESR parameters

Both plastocyanin and nitrosocyanin proteins host a copper II ion; therefore, they both are in a doublet spin state, bearing an unpaired electron formally attributed to the d^9 metal electronic configuration. However, the electron experiences quite an important delocalization over the ligands in both structures, even if the metallic character of the unpaired electron is much more pronounced in the case of nitrosocyanin, as confirmed by population analysis. This indicates that in the case of nitrosocyanin, one faces a less important, or less efficient, overlap between ligands and metal d orbitals. The computed ESR g-factors and hyperfine parameters reported in Table 1, which compare very well with experimental parameters [3, 29], show one dominant component of the diagonalized g-factor tensor and two smaller ones, similar between them, and greater than the free electron g-factor. This occurrence indicates a partial $d_{x^2-y^2}$ nature of the free electron in the ground state, coherent with DFT calculations that place such an orbital as the singly occupied molecular orbital. We can also notice that the value of the g-factor should be directly proportional to the amount of the d-character and inversely proportional to the ligand field energy difference between $d_{x^2-y^2}$ and d_{xy} orbitals [29]. Since the value of the computed g-factors are almost equal for both proteins, while the ligand field separation should be much higher, as confirmed spectroscopically by Basumalick et al. [29], we have another confirmation of the more pronounced metallic character of the ground state in nitrosocyanin.

3.3 Native protein UV/VIS and CD spectra

In Figs. 4 and 5, we report the TD-DFT computed spectra of wild-type plastocyanin and nitrosocyanin, respectively. One can immediately see that the UV/VIS spectrum of plastocyanin is dominated by the intense absorption at about 600 nm, responsible for the blue color of the protein; some weaker structures appear at shorter and longer

Table 1 Computed ESR g-factors and hyperfine A constants

	Plastocyanin	Nitrosocyanin
g_{xx}	2.059 (2.047)	2.037 (2.036)
g_{yy}	2.094 (2.059)	2.099 (2.059)
g_{zz}	2.185 (2.226)	2.225 (2.245)
A_y	30.3 G (|25| G)	51.5 G (|16| G)
A_z	−112.0 G (|177| G)	−138.7 G (|140| G)

Experimental results in parenthesis taken from [29]. Note that experimental techniques were not able to retrieve the sign of hyperfine A constant. Therefore, only the absolute value is given

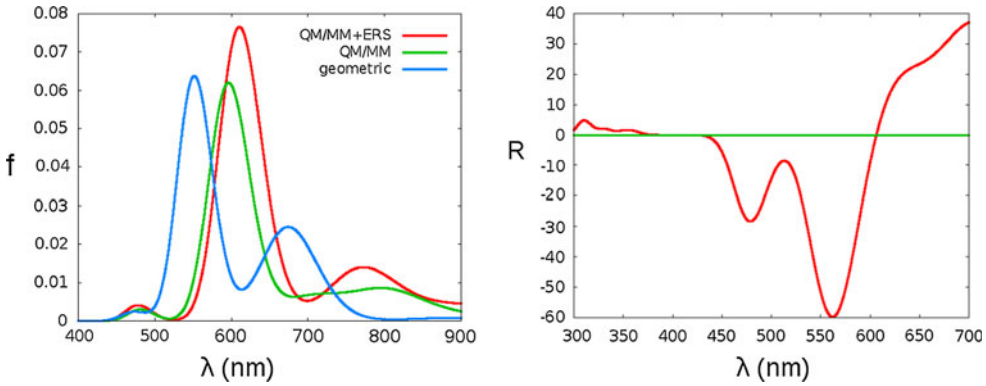

Fig. 4 The TD-DFT computed UV/VIS (*left*) and circular dichroism (*right*) spectra of plastocyanin. CD spectra are computed taking into account ERS polarization. Wavelengths in nm, intensities in arbitrary units. "QM/MM+ERS" stands for the QM/MM computation including polarization of the protein; "QM/MM" for the computation limited to electrostatic classical-quantum interactions and "geometric" means that the only geometric constrains are taken into account (the classical charges are switched off)

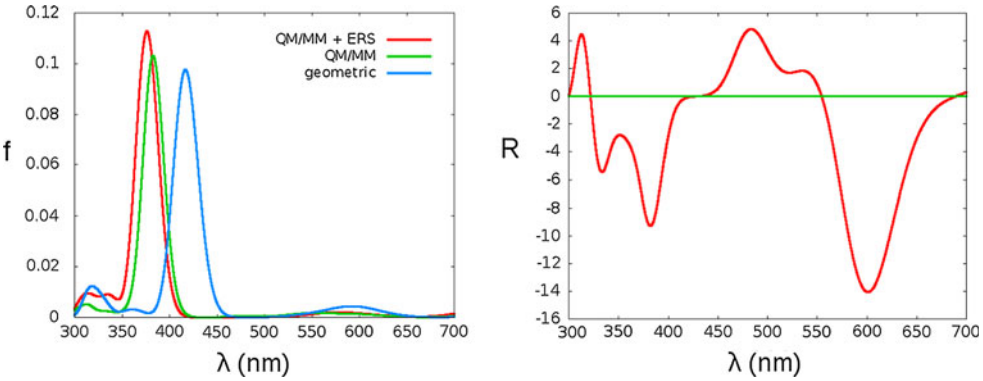

Fig. 5 The TD-DFT computed UV/VIS (*left*) and circular dichroism (*right*) spectra of nitrosocyanin. CD spectra are computed taking into account ERS polarization. Wavelengths in nm, intensities in arbitrary units. The notations are the same as for Fig. 4

wavelengths. As already stated on a previous paper [26], the UV/VIS spectrum matches well the experimental value [7] characterized by an absorption maximum at 598 nm. It also appears that the ERS effects, contrary to the electrostatic ones, do not have a very large magnitude although they enhance the intensity and modify the shape of the low-energy part of the spectrum. If one considers the CD spectrum, one can see that the presence of transitions in the region close to 550 nm is evidenced by a peak showing quite an important negative rotatory strength, and at the same time, the large band at 600 nm gives a very intense positive rotatory strength band. Notice also that now the region close to 450 nm is much better resolved than in the case of the UV/VIS spectrum. All these results are quite in agreement with the experimental ones (see for instance the works of Solomon [2]) reproducing all the main features of the CD spectrum, even if the intensities are in this case much more sensitive and, therefore, more difficult to reproduce at the same level of precision than for the UV/VIS spectra.

Contrarily to plastocyanin, nitrosocyanin exhibits a very strong absorption band centered at 380 nm, that compares very well with the experimental one centred at 390 nm [29], and which is responsible for the red color. We can also notice a very weak band at 500 nm, comparable to the experimental one centred at 491 nm, and two very large and weak bands, one around 570 nm (experimentally 568 nm) and a second one around 670 nm (experimental 666 nm). Again, the inclusion of ERS effect does not change too much the 390-nm band, even if the pure electrostatic treatment gives a peak red-shifted for about 20 nm, but the weak bands appear much more affected from the inclusion of polarization, in particular in the low-energy part of the spectrum. Finally, it must be emphasized that a treatment limited to the geometric deformation only is absolutely insufficient to quantitatively recover the spectrum features, the most intense band appearing, in this case, at 425 nm. As far as the CD spectrum is concerned, one can see an even more complicated structure when compared with the plastocyanin one. The 380-nm band gives rise to an intense CD band showing a negative rotatory strength. This compares well with experiment (see for instance Basumaick et al. [29]) although the calculated intensity for this band appears underestimated. Two bands

with positive rotatory strength at 490 and 550 nm are again identified in agreement with the experiment, as well as with some of the low intensity features already evidenced for the UV/VIS spectrum. Finally, one can identify the band at 600 nm, which shows a very intense negative rotatory strength; the latter can be directly compared with the band responsible of the blue color in the case of plastocyanin.

The different behavior of the two proteins can easily be rationalized by considering the NTOs (Fig. 6) for the most intense transition occurring at 600 and 390 nm for plastocyanin and nitrosocyanin, respectively. In both cases, the transition can be characterized as mainly a ligand (cytosine) to metal charge transfer, with a non-negligible participation of the other ligands. In the case of plastocyanin, however, the occupied NTO has a very strong π character while the main feature of nitrosocyanin appears as a σ antibonding interaction. It looks obvious that the change from one color to the other one takes place by enhancing the π or the σ metal to ligand charge transfer, respectively, while the less active transition undergoes a quenching of its intensity.

3.4 Plastocyanin mutations

Following the experimental works recently published on azurine by Clark et al. [13], we decided to selectively mutate the Met91 residue in spinach plastocyanin to assess for the different spectroscopic properties. The results for some of the most important bands are reported in Table 2. All the spectra reported there have been computed at the QM/MM level taking into account the ERS technique to model the response of the macromolecular environment.

The data fit very well experimental results reported by Clark et al. [13], even if care should be taken since in that work azurine protein was used instead, our results being able to correctly reproduce the variation of the absorption spectrum.

Notice the important effect due to the protonated or deprotonated state of the mutated cysteine, see also Fig. 7, and hence the strong dependence of the spectrum on the pH of the solution, a result again observed in the experimental study of mutated azurine [13].

It is also worth mentioning that in the case of glutamate mutation TD-DFT calculated spectrum presents also a second quite intense band at about 500 nm, as well as the band listed in Table 2. Note also that glutamate could show the same dependence with pH already evidenced for the cytosine mutant. Unfortunately, experimental data reported from Clark et al. [13] are not totally sufficient to entirely clarify this feature, as well as to clarify the pH dependence of the UV/VIS spectrum of such mutant.

Notice anyway that, as expected from the analysis of the structural parameters, the simple mutation of methionine

Table 2 Computed TD-DFT principal UV/VIS absorption transitions for the mutated Plastocyanin

	First band (nm)	Second band (nm)	Intensity ratio
Cys	589	452 (451)	2.00
Cys^-	526	447 (441)	0.44
Glu^-	550	440 (450)	0.66
Hcy^-	452	403 (410)	0.84

The aminoacid used to substitute the Meth91 residue is indicated a "–" indicates an anionic form. The values have been computed at QM/MM level including electronic response of the environment. In parenthesis experimental value for azurine taken from [13]

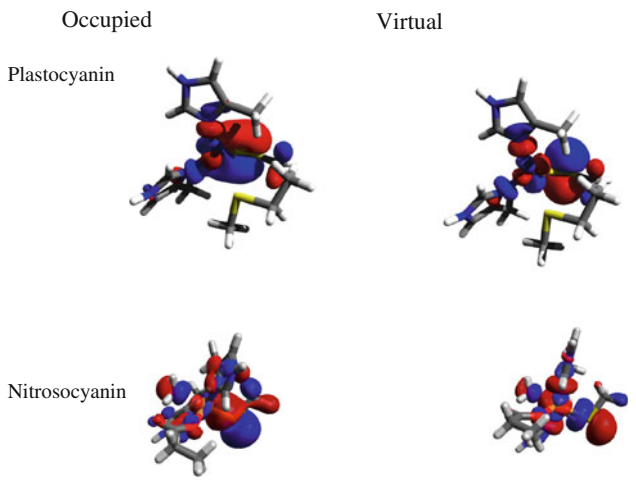

Fig. 6 NTOs for the most intense spectral band of plastocyanin (600 nm) and nitrosocyanin (390 nm)

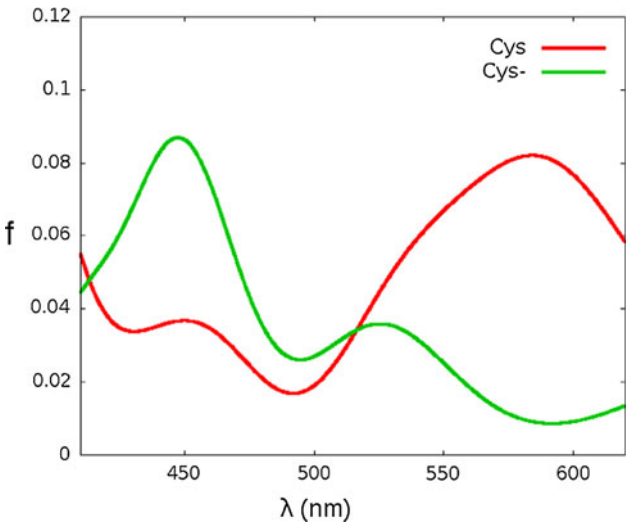

Fig. 7 The TDDFT spectrum of the mutated plastocyanin bearing a cysteine residue, in protonated and deprotonated state. Wavelengths in nm, intensities in arbitrary units

by a much stronger ligand like anionic cysteine is not sufficient to induce the change from a blue to a red protein, even if the spectrum is significantly altered and generally shifted to the short wavelengths. Indeed, the long distance between copper and the terminal sulfur atom imposed by the protein geometric constrain strongly limits the interaction strength. More flexible and extended ligands, such as glutamate and anionic homocysteine, on the other hand, produce a much more important shift. In particular with the mutation by the Hcy residue, this effect is so pronounced to be able to produce a red-copper protein.

4 Conclusions

We performed a systematic study of the structural and spectroscopic properties of two wild-type copper proteins: plastocyanin and nitrosocyanin and of mutated form of the first one.

In particular, optimized geometries, ESR parameters, UV/VIS, and CD spectra have been obtained, at QM/MM level, using DFT and TD-DFT techniques.

The different nature of the active site has been elucidated, as well as its influence on the spectroscopic properties, correctly reproducing experimental results, for the blue plastocyanin as well as for the red nitrosocyanin.

The UV/VIS spectra have also been analyzed to take into account the different effects produced by geometric deformation, electrostatic interactions, and polarization of the macromolecular moiety.

The nature of the excited states has been analyzed in terms of NTO showing how the main transition in the two proteins have a very different nature, one being based on a π interaction and the other on a σ one.

The effect of the mutation of the weak methionine ligand on the tetrahedral active site of plastocyanin has been studied, evidencing how the UV/VIS spectrum can be altered significantly by this mutation.

Again in coherence with experimental results on a similar azurine protein, we have shown how the mutation of only one ligand is able to induce the change from a blue to a red protein. The role of pH and of the protonation or deprotonation of the ligands has also been considered, as well as the influence of the lateral chain length of the mutated aminoacid. Indeed, because of the constrains by the protein backbone, when lateral chains are too short, they keep the electron donor atom too far away from the metal cation to produce a sufficiently strong interaction. The capability of reproducing such important and complex spectroscopic changes determined by a relative minor mutation can be considered as a significant proof of the robustness of our QM/MM methodology and strategy in the determination of excited state properties of biological molecules.

In the future, we plan to extend the present work in two directions: influence of solvation by a combined molecular dynamics (MD) and QM/MM study of the solvated proteins, and change in the properties of plastocyanin when all the amino acids of the active site are replaced by those of nitrosocyanin.

The first aspect is based on the run of a significantly long MD trajectory that will give access to the possible configuration assumed by the macromolecule and by its active site, and subsequently on the extraction of snapshots from the trajectory to compute the spectrum at the TD-DFT level. Even if the backbone of both copper proteins appears to be quite rigid, such a treatment will allow us to take into account many more effects, and in particular the role of local geometric modifications and the possible influence of the solvent.

The mutation of the whole active site aminoacid sequence will allow us to compare our findings with some very recent experimental data and to get even more insight on the role played by the macromolecular structure in finely tuning the rather particular and fascinating spectroscopic properties of these classes of proteins.

Acknowledgments Supports from Université de Lorraine and CNRS are gratefully acknowledged, also for the financing of the "chaire d'excellence" (A. M.). We also acknowledge support from the ANR project ANR-09-BLAN-0191-01 "PhotoBioMet".

References

1. Holm RH, Kennepohl P, Solomon EI (1996) Chem Rev 96:2239
2. Solomon EI, Hadt RG (2011) Coord Chem Rev 255:774
3. Solomon EI, Szilagyi RK, De Beer S, Basumallick G, Basumallick L (2004) Chem Rev 104:419
4. Gross EL (1993) Photosynth Res 37:103
5. Skyes AG (1991) Adv Inorg Chem 36:377
6. Mohamed MS, Fattah SA, Mostafa HM (2010) Curr Res J Biolog Sci 2:396
7. Book LD, Arnett DC, Hu H, Scherer NF (1998) J Phys Chem A 102:4350
8. Xue Y, Ökvist M, Hansson Ö, Young S (1998) Protein Sci 7:2099
9. Gewirth AA, Solomon EI (1998) J Am Chem Soc 110:3811
10. Nersissian AM, Nalbandyan RM (1988) Biochim Biophys Acta 957:446
11. Gray HB, Malström BG, Williams RJP (2000) J Biol Inorg Chem 5:551
12. Lockwood DM, Cheng Y-K, Rossky PJ (2001) Chem Phys Lett 345:159
13. Clark KM, YU Y, Marshall NM, Sieracki NA, Nilges MJ, Blackburn NJ, van der Donk WA, Lu Y (2010) J Am Chem Soc 132:10093
14. Ghosh S, Xie X, Dey A, Sun Y, Scholes CP, Solomon EI (2009) Proc Nat Acad Sci USA 106:4969
15. Ando K (2010) J Chem Phys 133:175101

16. Corni S, De Rienzo F, Di Felice R, Molinari E (2005) Int J Quant Chem 102:328
17. Ryde U, Olsson MHM, Pierloot K, Roos BO (1996) J Mol Biol 261:586
18. Olsson MHM, Ryde U (1999) J Biol Inorg Chem 4:654
19. Ryde U, Olsoon MHM (2001) Int J Quant Chem 81:335
20. Ando K (2004) J Phys Chem B 108:3940
21. Pierloot K, De Kerpel JOA, Ryde U, Olsson MHM, Roos BO (1998) J Am Chem Soc 120:13156
22. Sinnecker S, Neese F (2006) J Comput Chem 27:1463
23. Cascella M, Cuendet MA, Tavernelli I, Rohtlisberger U (2007) J Phys Chem B 111:10248
24. Le Bard DN, Matyushov DV (2008) J Phys Chem B 112:5218
25. Ando K (2008) J Phys Chem B 112:250
26. Monari A, Very T, Rivail J-L, Assfeld X (2011) Comp Theor Chem. doi:10.1016/j.comptc.2011.11.026
27. Lieberman RL, Arciero D, Hooper AB, Rosenzweig AC (2001) Biochemistry 40:5674
28. Arciero DM, Pierce BS, Hendrich MP, Hooper AB (2002) Biochemistry 41:1703
29. Basumalick L, Sarangi R, De Beer Giorgi S, Elmore B, Hooper AB, Hedmann B, Hodgson KO, Solomon EI (2004) J Am Chem Soc 127:3531
30. Besley NA, Robinson D (2011) Farady Discuss148:55
31. Berry SM, Bladhoim EL, Mostad EJ, Schenewerk AR (2011) J Biol Inorg Chem 16:473
32. Laurent AD, Assfeld X (2010) Interdiscip Sci Comput Life Sci 2:38
33. Loos P-F, Dumont E, Laurent AD, Assfeld X (2009) Chem Phys Lett 475:120
34. Jacquemin D, Perpète EA, Laurent AD, Assfeld X, Adamo C (2009) Phys Chem Chem Phys 11:1258
35. Dumont E, Laurent AD, Loos P-F, Assfeld X (2009) J Chem Theory Comput 5:1700
36. Ambrosek D, Loos P-F, Assfeld X, Daniel C (2010) J Inorg Biochem 104:893
37. Rodriguez-Ropero F, Zanuy D, Assfeld X, Aleman C (2009) Biomacromolecules 10:2338
38. Dreuw A, Head-Gordon M (2005) Chem Rev 105:4009
39. Frisch MJ, Trucks GW, Schlegel HB, Scuseria GE, Robb MA, Cheeseman JR, Scalmani G, Barone V, Mennucci B, Petersson GA, Nakatsuji H, Caricato M, Li X, Hratchian HP, Izmaylov AF, Bloino J, Zheng G, Sonnenberg JL, Hada M, Ehara M, Toyota K, Fukuda R, Hasegawa J, Ishida M, Nakajima T, Honda Y, Kitao O, Nakai H, Vreven T, Montgomery JA Jr, Peralta JE, Ogliaro F, Bearpark M, Heyd JJ, Brothers E, Kudin KN, Staroverov VN, Kobayashi R, Normand J, Raghavachari K, Rendell A, Burant JC, Iyengar SS, Tomasi J, Cossi M, Rega N, Millam NJ, Klene M, Knox JE, Cross JB, Bakken V, Adamo C, Jaramillo J, Gomperts R, Stratmann RE, Yazyev O, Austin AJ, Cammi R, Pomelli C, Ochterski JW, Martin RL, Morokuma K, Zakrzewski VG, Voth GA, Salvador P, Dannenberg JJ, Dapprich S, Daniels AD, Farkas Ö, Foresman JB, Ortiz JV, Cioslowski J, Fox DJ (2009) Gaussian 09, Revision A.1. Gaussian Inc., Wallingford, CT
40. Ferré N, Assfeld X, Rivail J-L (2002) J Comput Chem 23:610
41. Assfeld X, Rivail J-L (1996) Chem Phys Lett 266:100
42. Tinker code package: http://dasher.wustl.edu/tinker/
43. Brooks BR, Bruccoleri RE, Olafson BD, States DJ, Swaminathan S, Karplus M (1983) J Comput Chem 4:187
44. Hay PJ, Wadt WR (1985) J Chem Phys 82:270
45. Hay PJ, Wadt WR (1985) J Chem Phys 82:284
46. Hay PJ, Wadt WR (1985) J Chem Phys 82:299
47. Becke AD (1993) J Chem Phys 98:1372
48. Lee C, Yang W, Parr RG (1993) Phys Rev B 37:785
49. Runge E, Gross EKU (1984) Phys Rev Lett 52:997
50. Ditchfield R, Hehre WJ, Pople JA (1971) J Chem Phys 54:724
51. Hehre WJ, Ditchfield R, Pople JA (1972) J Chem Phys 56:2257
52. Rassolov VA, Ratner MA, Pople JA, Redfern PC, Curtiss LA (2001) J Comp Chem 22:976
53. Hansen E, Bak KL (1999) Enantiomer 4:455
54. Warnke I, Furche F, Wire Inter Rev. doi:10.1002/wcms.55
55. Yanai T, Tew D, Handy N (2004) Chem Phys Lett 393:51
56. Chai J-D, Head-Gordon M (2008) Phys Chem Chem Phys 10:6615
57. Adamo C, Barone VJ (1999) Chem Phys 110(110):6158
58. Martin RL (2003) J Chem Phys 118:4775